ACS Sustainable Chemistry & Engineering

pubs.acs.org/journal/ascecg

Research Article

Sized-Controlled ZIF-8 Nanoparticle Synthesis from Recycled Mother Liquors: Environmental Impact Assessment

Marta García-Palacín, José Ignacio Martínez, Lorena Paseta, Adam Deacon, Timothy Johnson, Magdalena Malankowska,* Carlos Téllez, and Joaquín Coronas*

Cite This: ACS Sustainable Chem. Eng. 2020, 8, 2973−2980

Read Online

ACCESS | Metrics & More | Article Recommendations | Supporting Information

ABSTRACT: The effect of different deprotonators as well as washing steps and drying procedure on the synthesis of ZIF-8 from the mother liquor was investigated. The morphology, thermal stability, crystallinity, and surface area of the synthesized MOF were investigated. In addition, life-cycle assessment (LCA) or, in other words, eco-balance, was implemented as well. LCA compares the full range of environmental effects associated with the product by evaluating all inputs and outputs of material flows and predicting how such flow will affect the environment. ZIF-8 nanocrystals were synthesized from the recycled mother liquors using NaOH or NH_4OH thus preserving the main characteristics of the ZIF-8 nanoparticles derived from the initial synthesis. The rest of the characterization methods confirmed the suitability of the synthesis methodology considering the phase purity of the obtained ZIF-8 and nanometer size particles. This procedure enabled us not only to obtain phase pure ZIF-8 but also to substantially decrease the amount of solvent used for washing making it a sustainable process.

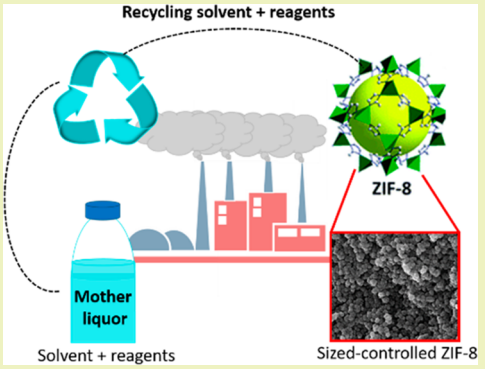

KEYWORDS: *ZIF-8, Mother liquor, MOF, Recycling, Particle size*

1. INTRODUCTION

Metal−organic frameworks (MOFs) are a growing class of crystalline and porous materials. They are formed by the self-assembly of complex subunits consisting of transition metal centers interconnected by various polyfunctional organic ligands in order to form 1D, 2D, or 3D structures.[1] They are characterized by high surface area and porosity, low density, and flexibility in pore size, shape, and structure. The presence of organic ligands in the MOFs enables good interaction with polymers, and they are commonly used in the preparation of mixed matrix membranes (MMMs).[2,3]

Zeolitic imidazolate frameworks (ZIFs) are a class of MOFs[4] that exhibit a zeolite type structure. They are characterized by high microporosity, exceptional chemical and thermal stability (up to 400 °C), and large surface area.[5,6] ZIFs are comprised of a divalent metal cation (i.e., Zn^{2+} or Co^{2+}) linked to the nitrogen atoms that are a part of a deprotonated imidazole molecule creating tetrahedral frameworks. In order to synthesize ZIFs, a different combination of not only metal cations but also imidazole linkers (i.e., 2-methylimidazolate, benzimidazolate) or solvents (water, ethanol, methanol, or dimethylformamide (DMF)) influences the properties, type, and structure of the resulting ZIF.[7] The above-mentioned stability combined with their regular microporous structures makes them very attractive for gas separations in adsorption[8] and membrane[9] applications.

ZIF-8 is the most well-known and studied type of ZIF. It is composed of the metal cation Zn^{2+} linked to the 2-methylimidazolate (mIm) ligand species resulting in large cavities of 1.16 nm interconnected through windows of about 0.34 nm.[7] A number of investigations have been carried out focusing on the synthesis of nanosized ZIF-8 crystals, varying the temperature, solvent, time of the reaction, and energy source.[10−13] The resulted ZIF-8 differs in size and crystallinity.[11,14] Recently, Jiang et al. developed a simple, one-step method to synthesize defect-free ZIF-8 films in aqueous solution by using dopamine as a modulator.[15]

Additionally, ZIF-8 can be synthesized mechanochemically which, besides being a sustainable process, has the benefit of short reaction times and a possibility of working at room temperature. The required mechanical impact is obtained by milling, shearing, grinding, scratching, or rapid friction. In this way, there is a chance to achieve a wasteless production of ZIF-8, something highly anticipated from an environmental protection point of view.[16] However, to the best of our knowledge, mechanosynthesis has not been able to produce

Received: December 19, 2019
Revised: January 24, 2020
Published: February 10, 2020

https://dx.doi.org/10.1021/acssuschemeng.9b07593
ACS Sustainable Chem. Eng. 2020, 8, 2973−2980

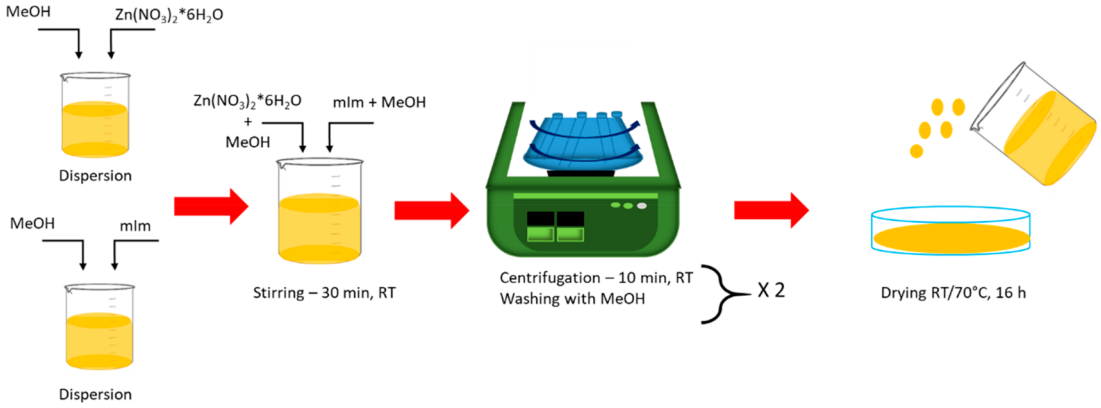

Figure 1. Synthesis of ZIF-8.

the particle size distribution (both narrow distribution and nanosize range) achieved by solvothermal processes.

After the synthesis of ZIF-8 nanocrystals, the mother liquor is anticipated to contain unreacted Zn^{2+}, mIm, and solvent (e.g., methanol). All these reagents may result in chemical waste and are costly to replace. An investigation of reagent (particularly solvents) recycling on the synthesis of MOFs is of crucial importance considering environmental and economic reasons.[17,18] Until now, attempts to synthesize ZIF-8 from recycled mother liquors were related to the use of sodium hydroxide or potassium hydroxide to initiate the nucleation and favor the crystal growth.[5,6,19] However, in this work, we demonstrate the synthesis of nanosized ZIF-8 from the recycled mother liquors maintaining constant particle size (that means the average particle sizes of the original ZIF-8 synthesis and those synthesized from mother liquors will be similar) and its specific surface area when also ammonia was used as deprotonator. In fact, ammonia has been shown to control the crystal texture and particle size during the synthesis of several ZIFs.[20,21] The morphology, thermal stability, crystallinity, and surface area of the synthesized MOF were investigated. In addition, life-cycle assessment (LCA) or, in other words, eco-balance, was implemented as well. LCA is a technique which is used to estimate the environmental impacts related to all the stages of product development, starting from raw material extraction through materials processing, manufacture, distribution, usage, maintenance, and finally disposal or recycling. LCA compares the full range of environmental effects associated with the product by evaluating all inputs and outputs of material flows and predicting how such a flow will affect the environment. Nowadays, the condition of the environment is dramatic and all scientific institutes and companies that are investigating or producing new materials have to take responsibility for their actions. Environmental protection and sustainable development are not optional; they are necessities. For instance, high solvent demand means energy-intensive recycling that contributes to global warming. In this work, we focus on minimizing the use of washing steps that will correspond to a decrease of the amount of solvent required to obtain high crystalline ZIF-8. The impact of this was evaluated by the estimation of the environmental effects, something never done before with MOF synthesis. Finally, we consider that the more sustainable synthesis of ZIF-8 may provide something like an "eco-label" to the new ZIF-8. This would make our MOF more desirable to the market for MOFs than others prepared by conventional, less sustainable methods.

2. MATERIALS AND METHODS

2.1. Materials. Zinc nitrate hexahydrate ($Zn(NO_3)_2 \cdot 6H_2O$, 98%) and 2-methyl imidazole (mIm, 99%) were obtained from Acros Organics. Sodium hydroxide (NaOH pellets, extra pure) was obtained from Scharlau, and ammonia (NH_3, 25% vol) was obtained from Panreac. All materials were used without any further purification. Methanol is considered as a problematic solvent in hazard ranking;[22] however, (i) it is not considered as hazardous as the DMF used in its early synthesis and (ii) allows the synthesis of activated ZIF-8.[23] Nevertheless, in the end, methanol was rated as "recommended", even though it is considered as "problematic" by default. In fact, its synthesis has a low energy-demand and it is very short. Moreover, the current occupational exposure limits for methanol are quite high including its ICH limit (3000 ppm). The ICH is the International Council for Harmonisation of Technical Requirements for Pharmaceuticals for Human Use that brings together regulatory authorities to discuss scientific and technical aspects of drug registration or guidelines for residual solvents.

2.2. Synthesis of ZIF-8 Crystals. In a typical synthesis, 2.933 g of zinc nitratehexahydrate ($Zn(NO_3)_2 \cdot 6H_2O$, 9.87 mmol) was dissolved in 200 mL of MeOH. A second solution consisting of 6.489 g of 2-methylimidazole (mIm, 79.04 mmol) in 200 mL of MeOH was prepared in parallel. The Zn^{2+} solution was rapidly poured into the mIm solution, and after 30 min of stirring at room temperature, ZIF-8 nanocrystals were recovered from the mother liquor by centrifuging at 8000 rpm for 15 min and washing twice with 50 mL of fresh MeOH. The final product was then dried overnight at either room temperature or 70 °C (Figure 1).

2.3. Synthesis of ZIF-8 Crystals from Recycled Mother Liquors. Following the crystallization, the mother liquor was separated from the nanocrystals by centrifugation and used again for the subsequent synthesis of ZIF-8. Our target was to replicate the exact same synthesis and obtain the nanocrystals as similar to the original ZIF-8 as possible considering the morphology and size of the nanoparticles.

To do that, once the crystals of the synthesis were separated, thermogravimetry was used to determine the percentage of pure ZIF-8 synthesized. The amount of unreacted reagents present in mother liquors was calculated by mass balance and the missing amount of those reagents was added. The yield of ZIF-8 was defined as the ratio of the amount of solid product obtained from 100 g of synthesis mixture to the maximum possible amount of ZIF-8 that can be produced from 100 g of synthesis mixture if all limiting reactant (Zn^{2+}) is consumed. To favor the crystallization yield, two different deprotonators were used: NaOH (procedure A) and NH_4OH (procedure B).

2.4. Characterization of ZIF-8. XRD powder patterns were acquired on a D-Max 2500 Rigaku X-ray diffractometer with a copper

https://dx.doi.org/10.1021/acssuschemeng.9b07593
ACS Sustainable Chem. Eng. 2020, 8, 2973−2980

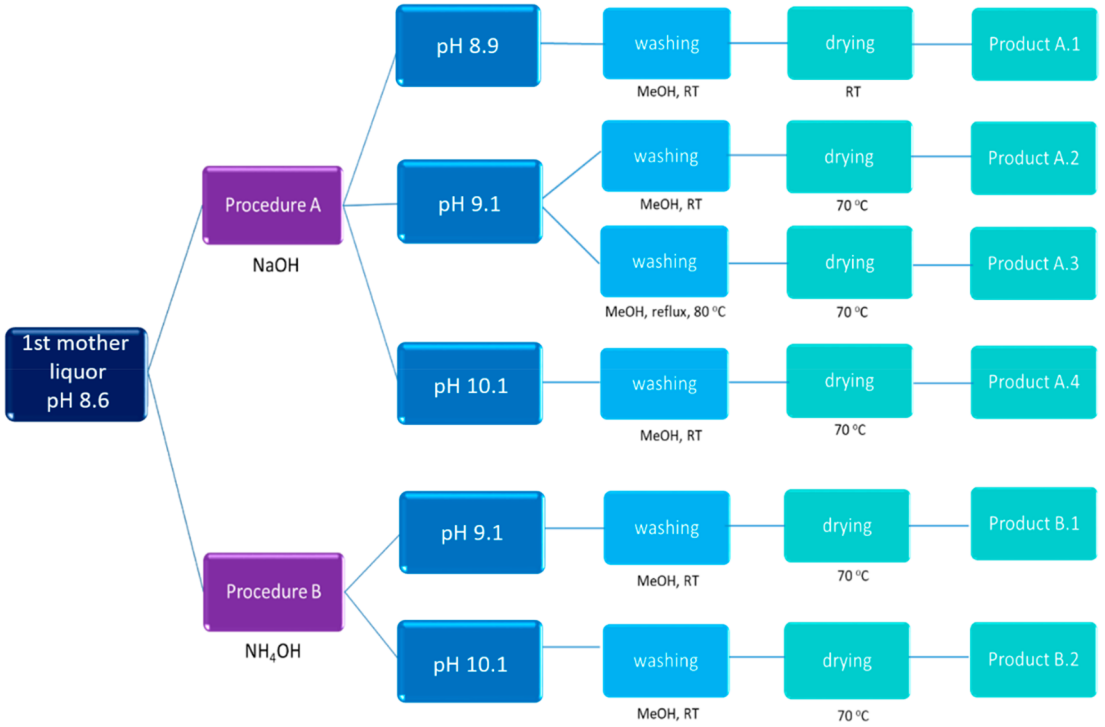

Figure 2. Schematic representation of the recycle of mother liquor.

anode and a graphite monochromator using Cu Kα radiation (λ = 1.540 Å), taking data from 2θ = 2.5° to 40° at a scan rate of 0.03°/s and operating parameters of 40 kV and 80 mA. Phase identification was conducted by comparison to simulated powder patterns.

The N_2 adsorption−desorption isotherms were obtained using a Micrometrics Tristar 3000 at 77 K. Before these measurements, ZIF-8 samples were degassed for 8 h under a vacuum at 200 °C using a heating rate of 10 °C/min. The surface area was calculated using the Brunauer−Emmett−Teller (BET) equation.

Thermal behavior was determined by thermogravimetric analysis (TGA) which was carried out using a Mettler Toledo TGA/STDA 851e. Samples (10 mg) placed in 70 μL alumina pans were heated under airflow of 40 mL/min between 35 and 900 °C with a heating rate of 10 °C/min.

Nanocrystal morphology and size were determined by scanning electron microscopy (SEM). The images were obtained using an Inspect F50 model scanning electron microscope (FEI) operating at 20 kV. The average particle size was determined using ImageJ 1.49b software, where at least 50 particles were counted for each sample.

2.5. Life-Cycle Assessment. Both the syntheses of ZIF-8 from fresh reactants and ZIF-8 from the recycled mother liquor were analyzed based on five different factors, focusing on the estimation of the key environmental impacts. Stoichiometric factor (SF) which considers an excess usage of some reagent in the process. Material recovery parameter (MRP) which examines, in general, the use of solvents, catalysts, and all products involved in the reaction and purification treatment. Reaction mass efficiency (RME) includes all the above factors giving a more general idea of the process sustainability. Atom economy (AE) shows the conversion efficiency of a chemical process in terms of all atoms involved and the desired products obtained. Finally, reaction yield (RY) was also considered for the correlation.

To visualize the process sustainability in a fast and simple way, Microsoft Excel was used. In this way, SF was calculated from eq1

$$\mathrm{SF} = \frac{\textit{excess reagents mass}}{\textit{stoichiometric reagents mass}} \tag{1}$$

AE was calculated from eq 2

$$\mathrm{AE} = \frac{\textit{Atoms products mass}}{\textit{Atoms reagents mass}} \tag{2}$$

MRP was calculated from eq 3

$$\mathrm{MRP} = \frac{1}{\left[1 + \left(\frac{\varepsilon * AE * (c+s+w)}{SF * mp}\right)\right]} \tag{3}$$

where ε means the RY expressed as parts per unit; c, the catalyst mass; s, the solvent mass; w, the post-treatment products mass; and mp, the final product mass.

RME factor was calculated from eq 4

$$\mathrm{RME} = \varepsilon * \mathrm{AE} * \frac{1}{SF} * MRP \tag{4}$$

Finally, the RY (%) was calculated from eq 5

$$\mathrm{RY} = \frac{\exp \cdot \mathrm{ZIF} - 8 - \left(\exp \cdot \mathrm{ZIF} - 8 * \left(\frac{\%\ \mathrm{mImef}}{100}\right)\right)}{\text{Theoretic ZIF} - 8} * 100 \tag{5}$$

where "exp. ZIF-8" is the mass of dry ZIF-8 collected after the synthesis. This includes both structural and extra-framework ligand (mIm). "% mIm" corresponds to extra-framework mIm, i.e., the TGA loss of weight observed from approximately 100 to 300 °C (Figure 4b). And "Theoretic ZIF-8" is the theoretic yield considering the limiting reagent and the empirical formula of ZIF-8, $Zn(mIm)_2$.

3. RESULTS AND DISCUSSION

3.1. Synthesis of ZIF-8. The crystallization of ZIF-8 at room temperature is fast, and it is anticipated that it will continue during the recovery of solid product during centrifugation. The synthesis of nanosized ZIF-8 requires fast nucleation with slow crystal growth during the crystallization process. Ligand mIm acts as a stabilizer in its neutral form and as a linker in its deprotonated form; hence, it has a dual function in the synthesis. The pH and the concentration of the deprotonated mIm decreases with an increase of the crystallization of ZIF-8. Low pH leads to the stabilization of

https://dx.doi.org/10.1021/acssuschemeng.9b07593
ACS Sustainable Chem. Eng. 2020, 8, 2973−2980

the neutral mIm, which as a result limits the rate of phase transformation. The neutral and protonated forms of mIm coexist in the solution at equilibrium.[6,10] This justifies the use of deprotonators to maintain a high value of pH and, consequently, increase the reaction to ZIF-8. The representative reaction for the synthesis of ZIF-8 is shown below

$$Zn(NO_3)_2 \cdot 6H_2O + 2C_4H_6N_2 \rightarrow Zn(C_4H_5N_2)_2 + 2H^+ + 2NO_3^- + 6H_2O$$

The reaction produces nitric acid, thus the pH of the medium decreases with crystallization. Low pH leads to the stabilization of the neutral mIm, which results in rate limitation of a phase transformation. A base added to the mother liquor will increase the pH, favoring deprotonation of the mIm. It will facilitate the initiation of nucleation and stimulate the crystal growth.[24] It should be noted that nitric acid, besides being corrosive (hindering the eventual use of vessels made of steel), in organic mixtures may be explosive. Nevertheless, by keeping the pH basic and by performing the synthesis at room temperature, both risks are mitigated.

The effect of the addition of two different bases was investigated: NaOH and NH_4OH. The initial pH of the solution was 9.1 which decreased down to 8.6 after 30 min of stirring.

Moreover, in order to make the synthesis process more sustainable, the effect of drying temperature and the frequency of washing was investigated as well. As shown in Figure 2, two procedures were considered using different bases to favor deprotonation of mIm followed by the study of the washing and drying procedures.

Figure 3 shows the XRD pattern of the as-synthesized ZIF-8 from fresh solution. Rietveld structural refinements were

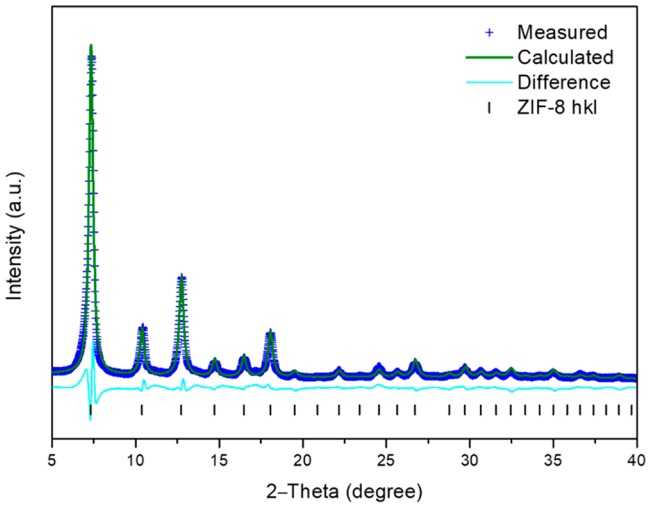

Figure 3. XRD pattern and subsequent Rietveld refinement of ZIF-8 produced from fresh synthesis solution.

conducted using the GSAS IIpackage.[25] Peak positions and relative intensity match well with single crystal data[26] corresponding to ZIF-8 (sod type structure). The final Rietveld refinement gave: $a = b = c = 16.939$ Å; $V = 4860.5$ Å^3; space group $I\text{-}43m$; $R_{wp} = 14.37\%$ (2θ range 5.0−39.98°; 2663 profile points; 57 refined variables; see Table S1 for the crystal lattice parameters, Table S2 for atom positions, and Table S3 for unit cell parameters calculated for the original synthesis). The reaction yield was 38%.

3.2. Synthesis of ZIF-8 from Recycled Mother Liquor.

The mother liquor, that contained a substantial amount of unused Zn^{2+} and mIm in methanol, due to the low conversion was recovered after the first synthesis. For the recycled, the base was added to the mother liquor to increase the pH value. Moreover, the missing amount of Zn^{2+} and mIm were added to the mixture, and after 30 min of stirring ZIF-8 nanocrystals were formed. Some differences could be observed when changing the conditions, as shown below.

Table 1 shows the main parameters of ZIF-8 that was originally synthesized and the recycled products A.1, A.2, A.3, A.4, B.1, and B.2. Zn^{2+}:base ratio, reaction yield, BET surface area and average particle size that was obtained after measuring the length of 50 particles from each sample from the SEM images.

Table 1. Main Parameters of ZIF-8 Originally Synthesized and Recycled Products[b]

Sample code		Zn^{2+}:base ratio	Yield (%)	BET surface area (m^2/g)	Average particle diameter (nm)
	ZIF-8		38 ± 2[a]	1773 ± 17	31
NaOH	A.1	1:2	37	515 ± 9	27
	A.2	1:4	27	826 ± 7	13
	A.3	1:4	24 ± 1[a]	1620 ± 14	18
	A.4	1:10	62	1420 ± 9	33
NH_4OH	B.1	1:18	43	1713 ± 12	18
	B.2	1:54	65	1543 ± 15	18

[a]Mean and standard deviation from experimental repetition. [b]Zn^{2+}:base ratio, reaction yield, BET surface area, and average particle diameter.

3.2.1. NaOH As a Base (Procedure A). To increase the pH value from 8.6 to 9.1, NaOH was added to the mother liquor and the mixture was stirred until the NaOH was dissolved. In all cases, the amounts of Zn^{2+} and mIm added to the mixture were previously calculated from thermogravimetry results. The mIm trapped in the structural pores (extra-framework ligand) and the structural mIm percentages were obtained from the 100−300 °C and 300−600 °C respective temperature ranges from the TGA synthesis curves in Figure 4B. Figure S1 in the Supporting Information shows the 2-methylimidazole decomposition curve analyzed by thermogravimetry (removed below 250 °C) for an easier correlation.

In the same way, the effect of a higher pH than 9.1 on the crystallinity, morphology, and particle size was also investigated by varying the NaOH amount added and repeating the same steps leading to the formation of products A.1 to A.4 (see Figure 2).

For product A.1, the amount of added base was calculated as the stoichiometric amount of base per mol of generated protons in the synthesis reaction, showing a 1:2 Zn^{2+}/NaOH ratio. As Figure S2 depicts, the XRD pattern of product A.1 contains an impurity. Extra phase is indexable to ZIF-L. Weight percentages of the two phases calculated from the refinement in A.1 were 27 wt % of ZIF-8 and 73 wt % of ZIF-L (see Tables S4 and S5 for atom positions and unit cell parameters of ZIF-8, respectively, and Tables S6 and S7 for atom positions and unit cell parameters for ZIF-L, respectively). The BET area

https://dx.doi.org/10.1021/acssuschemeng.9b07593
ACS Sustainable Chem. Eng. 2020, 8, 2973−2980

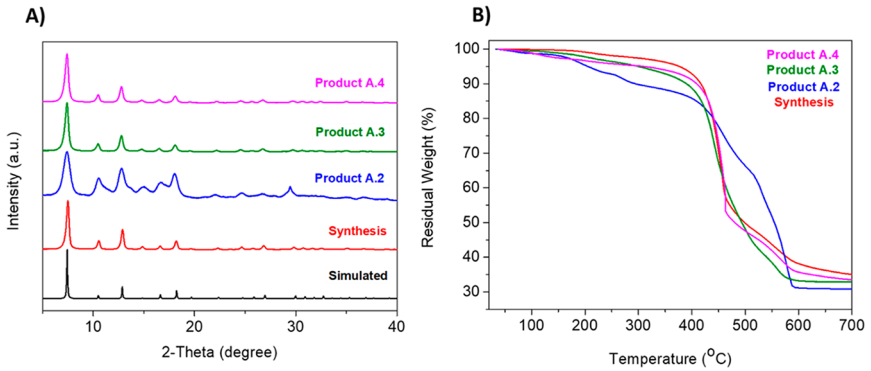

Figure 4. ZIF-8 synthesis and products A.2-A.4 using NaOH as base: (A) XRD patterns; (B) TGA curves.

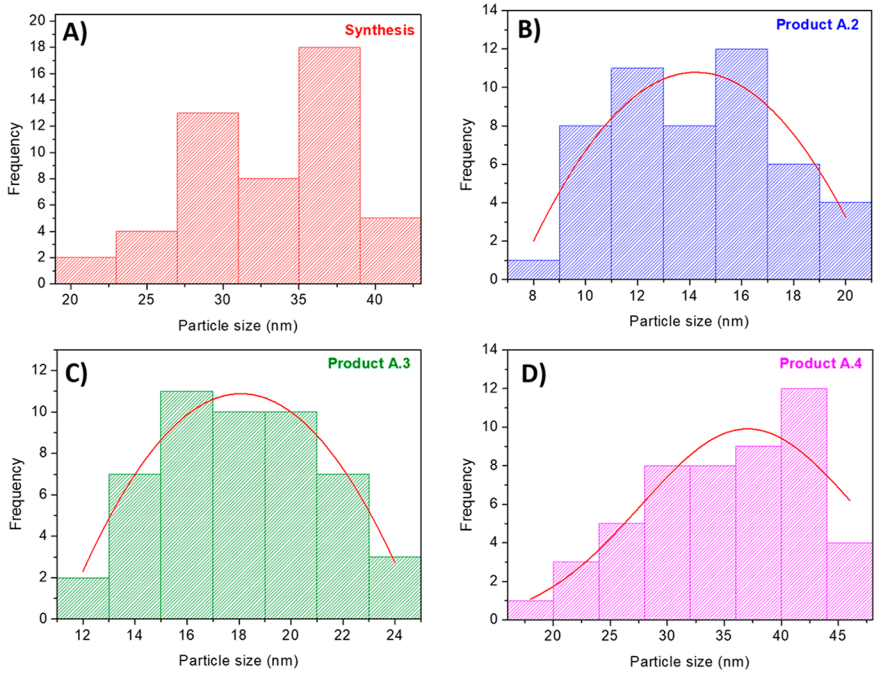

Figure 5. Particle size distributions of the (A) synthesis, (B) product A.2, (C) product A.3, and (D) product A.4.

was smaller, 515 m^2/g, than the expected for ZIF-8 (see Table 1). These results may be due to the pH value of 8.6, which was perceptibly lower than the initial value of 9.1.

In view of the results, the synthesis solution was titrated by addition of NaOH pellets (to avoid any additional dilution of the reaction media) until the pH was raised up to 9.1 and products A.2, A.3, and A.4 were formed; with a Zn^{2+}/NaOH ratio of 1:4 for products A.2 and A.3 and 1:10 for product A.4. XRD patterns show that by re-establishing the pH value, the previous impurity was not formed (Figure 4a).

The change between different products was focused on the washing step as well as the drying temperature. Product A.2 was washed with free MeOH at room temperature, while product A.3 was washed with MeOH under reflux and dried at 70 °C. This difference can be observed both in the XRD pattern and in the TGA curves (Figure 4b). XRD pattern shows that product A.3 possesses more crystallinity (narrower peaks) than A.2 due to reflux used in the A.3 product washing step. Figure S3 depicts the peak fitting of product A.3, and Tables S8 and S9 show atom positions and unit cell parameters, respectively; once more, peak positions and relative intensity match well with the sod type structure of ZIF-8. Reflux improved the release of mIm occluded in the structural ZIF-8 pores compared to a simple wash with fresh MeOH. Because of this, the percentage of extra-framework mIm in the TGA curve (related to the step at ca. 275 °C) was less pronounced for product A.3. Additionally, the BET surface area increased from 826 to 1620 m^2/g due to the absence of mIm in the pores (Figure S4 and Table 1).

Once the pH was controlled at 9.1, the same experiments were reproduced with increasing the pH value to a higher one and trying not to use reflux to make the process more sustainable. The amount of MeOH used for both reflux and free methanol washing was always kept the same for the comparison. The resulting product, A.4, was formed but the XRD and TGA characterization results did not change significantly (see Figure 4). Only the reaction yield rose from 30% to 70% when the pH value increased from 8.6 to 10.1. However, the surface area determined by BET decreased slightly from 1620 to 1420 m^2/g. Moreover, the particle sizes of all synthesized products, measured from SEM images, reveal that the mean size is relatively constant (13−33 nm) and, especially in the case of product A.4, the particle size is very

https://dx.doi.org/10.1021/acssuschemeng.9b07593
ACS Sustainable Chem. Eng. 2020, 8, 2973−2980

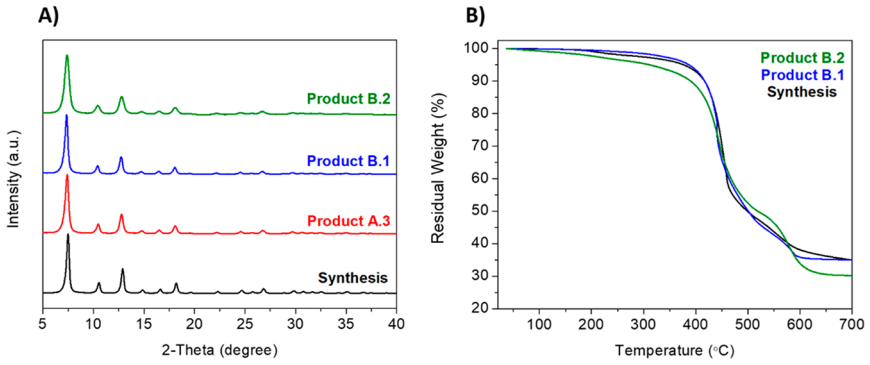

Figure 6. ZIF-8 synthesis and products B.1-B.2 using NH_4OH as base: (A) XRD patterns; (B) TGA curves.

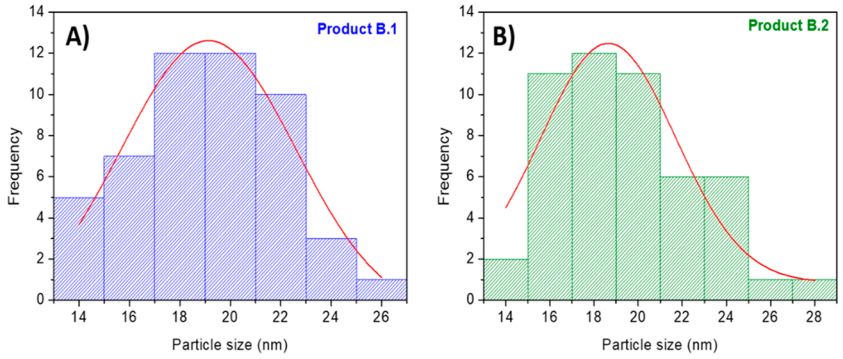

Figure 7. Particle size distribution of the (A) product B.1 and (B) product B.2.

close to that in the original synthesis (approximately 33 nm) (see Figure 5 and Table 1 for details).

It was concluded that reflux and elevated temperature was necessary in order to obtain material that will be the most like the original ZIF-8 synthesized in procedure A.

3.2.2. NH_4OH As a Base (Procedure B). To increase the pH value from 8.6 to 9.1 or 10.1, NH_4OH, a weaker base than NaOH, was added to the mother liquor (see Figure 2) and the mixture was stirred until it was dissolved. When the pH value was returned to 9.1, product B.1 was formed with a Zn^{2+}/NH_4OH ratio of 1:18. The washing step consisted of a simple wash with fresh MeOH. XRD patterns and TGA curves of products B.1, B.2, and a comparison to the best product obtained in procedure A (A.3) are shown in Figure 6. As compared to the products obtained with NaOH, the use of the deprotonator NH_4OH did not give rise to ZIF-L and produced TGA curves with almost no weight loss at ca. 275 °C (related to the ligand).

With a re-established pH of 9.1, product B.1 differed from the product A.3 by the washing step. To obtain similar final characteristics, product A.3 was washed under reflux while product B.1 only needed a simple wash. In addition, high BET surface areas of both ZIF-8 recycled samples, i.e., A.3 and B.1 (1620 m^2/g and 1713 m^2/g, respectively), similar to the ZIF-8 original synthesis product (1773 m^2/g), prove that the crystals possess fully developed microstructure with high crystallinity (see Figure S5) and uniform nanoparticle size, i.e., 18 nm (see Figure 7).

The reaction yield (43%) was also higher for the product B.1 than for A.3 (24%); thus, it was concluded that procedure B (NH_4OH as a base) was more sustainable than procedure A, since it did not need any additional washing under reflux and high temperature (see Figure S6 for comparison).

When the pH value increased above 9.1, product B.2 was formed. In this case, the reaction yield increased (from 43% corresponding to product B.1 up to 65% for product B.2), as it happened in procedure A, and BET area diminished (Figure S5, Table 1). This suggests that there is an optimal pH value for which the BET surface area exhibits its maximum, maintaining good XRD and TGA results (no extra-framework ligand) and morphology. Figure 8 shows the SEM images of all the products obtained in this work.

Finally, it is worth mentioning that deprotonators act over the ligand availability favoring the reaction yield and this was macroscopically observed through SEM, XRD, and adsorption characterizations and yield calculations. However, the microscopic phenomena that occur at molecular level should not be different from those observed by other authors in the synthesis of ZIF-8. In fact, Cravillon et al.[27] claimed that the crystallization of ZIF-8 exhibits similarities to crystallization processes of other chemical systems, for example, zeolites.

To establish a methodology of green metrics for the synthesis of MOFs, product A.3 was subjected to deeper study. Thus, both synthesis and recycled green metrics factors were calculated using the formulas shown in the experimental section. In the recycled solutions, the calculation was done by the sum of all quantities added from the beginning, accounting for up to five successive recycling processes. The results were represented as a radial pentagon diagram the axes of which emanated from center and belonged to each one of the five factors involved; 1 being the value of the factor for an ideal process (Figure 9). This figure shows the A.3 product evolution along the recycled cycle. As expected, the reaction yield (RY) increased along with the inverse of the stoichiometric factor (1/SF). This is due to a decrease in excess reagents, and the same solution from the original

https://dx.doi.org/10.1021/acssuschemeng.9b07593
ACS Sustainable Chem. Eng. 2020, 8, 2973−2980

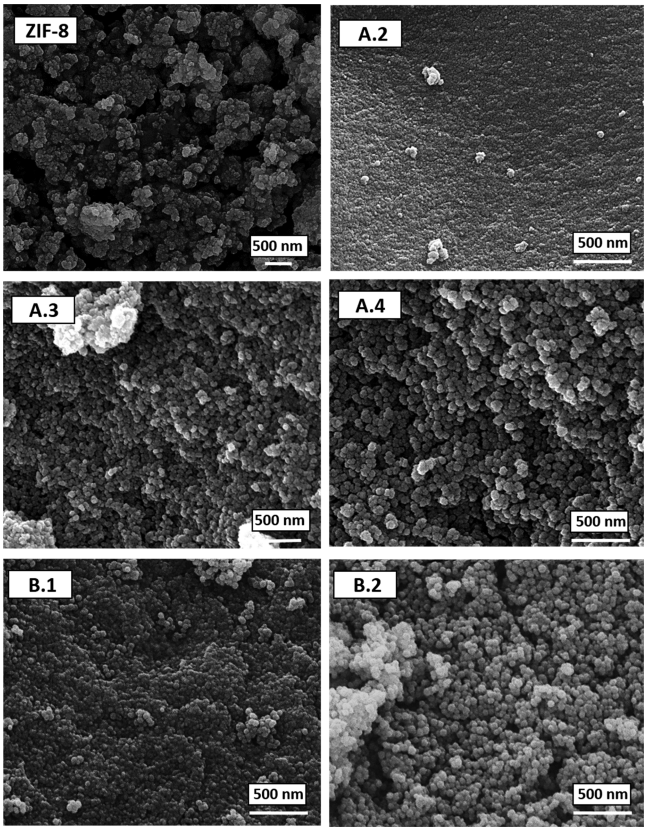

Figure 8. SEM images of ZIF-8 from original synthesis (ZIF-8) and products A.2, A.3, A.4, B.1, and B.2 synthesized from mother liquors.

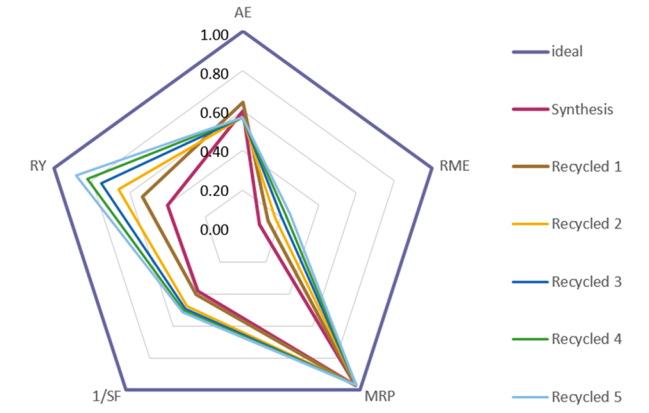

Figure 9. Green metrics in ZIF-8 synthesis, ideal and recycled ZIF-8 from procedure A.3.

synthesis was used. Analogously, the reaction mass efficiency factor (RME) was improved with recycling, since it included the above factors. The atom economy (AE) decreased due to the addition of NaOH which increased the mass reagent atoms. This parameter and the material recovery parameter (MRP) were the least affected by the recycling methodology implemented in this work. Nevertheless, parameters RY, RME, and 1/SF showed clear improvements justifying the increase of AE due to the necessary contribution of the inorganic base to the greener synthesis process (see Table S10 for details of each recycling step).

4. CONCLUSION

ZIF-8 nanocrystals were synthesized from recycled mother liquors using NaOH or NH_4OH thus preserving the main characteristics of the ZIF-8 nanoparticles derived from the initial synthesis. In fact, when the synthesis parameters were optimized, the activated ZIF-8 was directly produced from the methanol synthesis with a BET specific surface area of ca. 1700 m^2/g. The best performance was achieved with NH_4OH as deprotonator; in fact, NH_4OH was preferred over NaOH to re-establish the pH value (9.1) due to the possibility of avoiding the high temperature reflux-wash that must be applied in the case of the NaOH procedure. The rest of the characterization methods confirmed the suitability of the synthesis methodology considering the phase purity of the obtained ZIF-8 (as determined by XRD) and nanometer size particles (average sizes in the range of 13−31 nm).

The eco-balance methodology applied, consisting of the calculation of up to five different indicators, allowed us to conclude that certain parameters (reaction yield, above all, inverse of the stoichiometric factor and reaction mass efficiency) were progressively enhanced along five successive recycling processes, while atom economy, which in fact decreased due to the addition of inorganic base, and material recovery parameters were not improved. Interestingly, the NH_4OH procedure proved to be a greener process than the NaOH procedure with better results.

■ ASSOCIATED CONTENT

Supporting Information

The Supporting Information is available free of charge at https://pubs.acs.org/doi/10.1021/acssuschemeng.9b07593.

Detailed data for XRD patterns obtained from Reitveld refinement (crystal lattice parameters, atom positions, and unit cell parameters), N_2 adsorption and desorption isotherms, thermogravimetric comparison of products A.2 and B.1 as well as TGA of mIm, values for green metric factors for each recycling step in product A.3 (PDF)

■ AUTHOR INFORMATION

Corresponding Authors

Magdalena Malankowska − *Chemical and Environmental Engineering Department, Instituto de Nanociencia de Aragón (INA) and Instituto de Materiales de Aragón (ICMA), Universidad de Zaragoza-CSIC, 50018 Zaragoza, Spain;* orcid.org/0000-0001-9595-0831; Email: magnal@unizar.es

Joaquín Coronas − *Chemical and Environmental Engineering Department, Instituto de Nanociencia de Aragón (INA) and Instituto de Materiales de Aragón (ICMA), Universidad de Zaragoza-CSIC, 50018 Zaragoza, Spain;* orcid.org/0000-0003-1512-4500; Email: coronas@unizar.es

Authors

Marta García-Palacín − *Chemical and Environmental Engineering Department, Instituto de Nanociencia de Aragón (INA) and Instituto de Materiales de Aragón (ICMA), Universidad de Zaragoza-CSIC, 50018 Zaragoza, Spain*

José Ignacio Martínez − *Chemical and Environmental Engineering Department, Instituto de Nanociencia de Aragón (INA) and Instituto de Materiales de Aragón (ICMA), Universidad de Zaragoza-CSIC, 50018 Zaragoza, Spain*

https://dx.doi.org/10.1021/acssuschemeng.9b07593
ACS Sustainable Chem. Eng. 2020, 8, 2973−2980

Lorena Paseta − *Chemical and Environmental Engineering Department, Instituto de Nanociencia de Aragón (INA) and Instituto de Materiales de Aragón (ICMA), Universidad de Zaragoza-CSIC, 50018 Zaragoza, Spain*
Adam Deacon − *Johnson Matthey Technology Centre, Billingham TS23 1LB, United Kingdom*
Timothy Johnson − *Johnson Matthey Technology Centre, Reading RG4 9NH, United Kingdom*
Carlos Téllez − *Chemical and Environmental Engineering Department, Instituto de Nanociencia de Aragón (INA) and Instituto de Materiales de Aragón (ICMA), Universidad de Zaragoza-CSIC, 50018 Zaragoza, Spain;* orcid.org/0000-0002-4954-1188

Complete contact information is available at: https://pubs.acs.org/10.1021/acssuschemeng.9b07593

Notes

The authors declare no competing financial interest.

■ ACKNOWLEDGMENTS

This project has received funding from the European Union's Horizon 2020 research and innovation program under grant agreement No 760944 (MEMBER project). Also, financial support from the Spanish Ministry of Science, Innovation and Universities and FEDER (MAT2016-77290-R), the Aragón Government (T43-17R) and the ESF is gratefully acknowledged. All the microscopy work was done in the Laboratorio de Microscopías Avanzadas at the Instituto de Nanociencia de Aragón (LMA-INA). Finally, the authors acknowledge the use of the Servicio General de Apoyo a la Investigación-SAI (Universidad de Zaragoza).

■ REFERENCES

(1) Férey, G. Hybrid porous solids: past, present future. *Chem. Soc. Rev.* **2008**, *37*, 191−214.
(2) Lin, R.; Villacorta Hernandez, B.; Ge, L.; Zhu, Z. Metal organic framework based mixed matrix membranes: an overview on filler/polymer interfaces. *J. Mater. Chem. A* **2018**, *6* (2), 293−312.
(3) Jiang, X.; Li, S.; He, S.; Bai, Y.; Shao, L. Interface manipulation of CO_2-philic composite membranes containing designed UiO-66 derivatives towards highly efficient CO_2 capture. *J. Mater. Chem. A* **2018**, *6*, 15064−15073.
(4) Sánchez-Laínez, J.; Zornoza, B.; Friebe, S.; Caro, J.; Cao, S.; Sabetghadam, A.; Seoane, B.; Gascon, J.; Kapteijn, F.; Le Guillouzer, C.; Clet, G.; Daturi, M.; Téllez, C.; Coronas, J. Influence of ZIF-8 particle size in the performance of polybenzimidazole mixed matrix membranes for pre-combustion CO_2 capture and its validation through interlaboratory test. *J. Membr. Sci.* **2016**, *515*, 45−53.
(5) Sahin, F.; Topuz, B.; Kalipcilar, H. Synthesis of ZIF-7, ZIF-8, ZIF-67 and ZIF-L from recycled mother liquors. *Microporous Mesoporous Mater.* **2018**, *261*, 259−267.
(6) KeserDemir, N.; Topuz, B.; Yilmaz, L.; Kalipcilar, H. Synthesis of ZIF-8 from recycled mother liquors. *Microporous Mesoporous Mater.* **2014**, *198*, 291−300.
(7) Park, K. S.; Ni, Z.; Côté, A. P.; Choi, J. Y.; Huang, R.; Uribe-Romo, F. J.; Chae, H. K.; O'Keeffe, M.; Yaghi, O. M. Exceptional chemical and thermal stability of zeoliticimidazolate frameworks. *Proc. Natl. Acad. Sci. U. S. A.* **2006**, *103* (27), 10186−10191.
(8) Sorribas, S.; Zornoza, B.; Téllez, C.; Coronas, J. Ordered mesoporous silica-(ZIF-8) core-shell spheres. *Chem. Commun.* **2012**, *48* (75), 9388−90.
(9) Bux, H.; Liang, F.; Li, Y.; Cravillon, J.; Wiebcke, M.; Caro, J. Zeolitic Imidazolate Framework Membrane with Molecular Sieving Propertiesby Microwave-Assisted Solvothermal Synthesis. *J. Am. Chem. Soc.* **2009**, *131* (44), 16000−16001.
(10) Cravillon, J.; Münzer, S.; Lohmeier, S. J.; Feldhoff, A.; Huber, K.; Wiecke, M. Rapid Room-Temperature Synthesis and Characterization of Nanocrystals of a Prototypical Zeolitic Imidazolate Framework. *Chem. Mater.* **2009**, *21* (8), 1410−1412.
(11) Pan, Y.; Liu, Y.; Zeng, G.; Zhao, L.; Lai, Z. Rapid synthesis of zeoliticimidazolate framework-8 (ZIF-8) nanocrystals in an aqueous system. *Chem. Commun.* **2011**, *7*, 2071−2073.
(12) Bao, Q.; Lou, Y.; Xing, T.; Chen, J. Rapid synthesis of zeoliticimidazolate framework-8 (ZIF-8) in aqueous solution via microwave irradiation. *Inorg. Chem. Commun.* **2013**, *37*, 170−173.
(13) Cho, H.-Y.; Kim, J.; Kim, S.-N.; Ahn, W.-S. High yield 1-L scale synthesis of ZIF-8 via a sonochemical route. *Microporous Mesoporous Mater.* **2013**, *169*, 180−184.
(14) Ordoñez, M. J. C.; Balkus, K. J., Jr; Ferraris, J. P.; Musselman, I. H. Molecular sieving realized with ZIF-8/Matrimid® mixed-matrix membranes. *J. Membr. Sci.* **2010**, *361*, 28−37.
(15) Jiang, X.; Li, S.; Bai, Y.; Shao, L. Ultra-facile aqueous synthesis of nanoporouszeoliticimidazolate framework membranes for hydrogen purification and olefin/paraffin separation. *J. Mater. Chem. A* **2019**, *7*, 10898−10904.
(16) Bennett, T. D.; Cao, S.; Tan, J. C.; Keen, D. A.; Bithell, E. G.; Beldon, P. J.; Friscic, T.; Cheetham, A. K. Facile mechanosynthesis of amorphous zeoliticimidazolate frameworks. *J. Am. Chem. Soc.* **2011**, *133*, 14546−14549.
(17) Gökpinar, S.; Diment, T.; Janiak, C. Environmentally benign dry-gel conversions of Zr-based UiO metal-organic frameworks with high yield and the possibility of solvent re-use. *Dalton Transactions.* **2017**, *46*, 9895−9900.
(18) Tannert, N.; Gökpinar, S.; Hastürk, E.; Nießing, S.; Janiak, C. Microwave-assisted dry-gel conversion-a new sustainable route for the rapid synthesis ofmetal-organic frameworks with solvent re-use. *Dalton Transactions.* **2018**, *47* (29), 9850−9860.
(19) Jamil, N.; Alias, N. H.; Shahruddin, M. Z.; Othman, N. H. A green *In situ* synthesis of hybrid Graphene-based zoeliticimidazolate framework-8 nanofillers using recycling mother liquor. *Key Eng. Mater.* **2019**, *797*, 48−54.
(20) Shi, Q.; Song, Z.; Kang, X.; Dong, J. Controlled synthesis of hierarchical zeoliticimidazolate framework-GIS(ZIF-GIS) architectures. *CrystEngComm* **2012**, *14*, 8280−8285.
(21) Venna, S. R.; Jasinski, J. B.; Carreon, M. A. Structural evolution of zeoliticimidazolate framework-8. *J. Am. Chem. Soc.* **2010**, *132*, 18030−18033.
(22) Prat, D.; Wells, A.; Hayler, J.; Sneddon, H.; McElroy, C. R.; Abou-Shehada, S.; Dunn, P. J. CHEM21 selection guide of classical- and less classical-solvents. *Green Chem.* **2016**, *18*, 288−296.
(23) Park, K. S.; Ni, Z.; Côté, A. P.; Choi, J. Y.; Huang, R.; Uribe-Romo, F. J.; Chae, H. K.; O'Keeffee, M.; Yaghi, O. M. Exceptional chemical and thermal stability of zeoliticimidazolate frameworks. *Proc. Natl. Acad. Sci. U. S. A.* **2006**, *103*, 10186−10191.
(24) Yeung, H. H.-M.; Sapnik, A. F.; Massingberd-Mundy, F.; Gaultois, M. W.; Wu, Y.; Fraser, D. A. X.; Henke, S.; Pallach, R.; Heidenreich, N.; Magdysyuk, O. V.; Vo, N. T.; Goodwin, A. L. Control of Metal-Organic Framework Crystallization by Metastable Intermediate Pre-equilibrium Species. *Angew. Chem., Int. Ed.* **2019**, *58*, 566−571.
(25) Toby, B. H.; Von Dreele, R. B. GSAS-II: the genesis of a modern open-source all purpose crystallography software package. *J. Appl. Crystallogr.* **2013**, *46*, 544−549.
(26) Karagiaridi, O.; Lalonde, M. B.; Bury, W.; Sarjeant, A. A.; Farha, O. K.; Hupp, J. T. Opening ZIF-8: A Catalytically Active Zeolitic Imidazolate Framework of Sodalite Topology with Unsubstituted Linkers. *J. Am. Chem. Soc.* **2012**, *134*, 18790−18796.
(27) Cravillon, J.; Schröder, C. A.; Nayuk, R.; Gummel, J.; Huber, K.; Wiebcke, M. Fast Nucleation and Growth of ZIF-8 Nanocrystals Monitored by Time-Resolved In Situ Small-Angle and Wide-Angle X-Ray Scattering. *Angew. Chem., Int. Ed.* **2011**, *50*, 8067−8071.